Biol. Cell (2007) **99**, 519–530 (Printed in Great Britain) doi:10.1042/BC20070026

online data

Research article

# Firing of transcription and compartmentalization of splicing factors in tomato radicle nuclei during germination[1]

**Olga Echeverría*, Gerardo Vázquez-Nin*, Silvia Juárez-Chavero* and Susana Moreno Díaz de la Espina†[2]**

*Departamento de Biología Celular, Facultad de Ciencias, UNAM, México DF, México, and †Laboratorio de Matriz Nuclear, Departamento de Biología de Plantas, Centro Investigaciones Biológicas, CSIC, Ramiro de Maeztu 9, 28040 Madrid, Spain

*Background information.* Germination is a well-characterized process in which embryo cells of seeds experience a programmed transition from quiescence to proliferation. For this reason they constitute a very good system to analyse nuclear evolution from a dehydrated practically inactive state until the steady state of proliferation. We analysed the temporal and spatial organization of transcription and splicing factors in nuclei of tomato radicle cells during germination. To address this issue we performed *in situ* immunodetection of several markers of these processes: the Z-DNA stretches forming behind the active RNA polymerases, the splicing proteins U2B″ and Sm, and the trimethyl guanosin cap of small nuclear RNA. The concomitant structural changes of the different nuclear compartments were studied in meristematic nuclei by electron microscopy and high-resolution cytochemistry for DNA and ribonucleoproteins.

*Results.* In quiescent cells practically no Z-DNA stretches were detected and splicing components localized mainly to one or two Cajal bodies associated to the nucleolus. In early germination, a massive de-condensation of chromatin and nucleolar Z-DNA conformation stretches were first detected, followed by the relocation of scarce splicing components to the small interchromatin spaces. Nucleoplasmic Z-DNA stretches were not detected until 4 h of imbibition and were accompanied by an important increase of splicing components in this nuclear domain. Soon after the post-germination stage, transcription and splicing topology and nuclear organization in meristematic nuclei resemble those in steady state growing tomato roots.

*Conclusions*. Our results demonstrate that, in tomato, dormant nuclei splicing factors are stored in nucleolar Cajal bodies. In early germination, RNA polymerase I transcription is first activated, whereas mRNA transcription is fired later and is accompanied by a massive de-condensation of chromatin and accumulation of splicing factors in the interchromatin domains. Nucleoplasmic Cajal bodies appear later in germination.

## Introduction

The cell nucleus has functional subdomains for gene silencing, replication, transcription and splicing that play roles in the organization of the different enzymatic machineries and also in gene expression (Spector, 2001). Besides the nucleolus, a multifunctional domain involved in pre-rRNA biosynthesis, the best-characterized of those related with splicing of pre-mRNAs are the nuclear speckles and CBs (Cajal bodies). The splicing factors are enriched in dynamic nuclear speckles that correspond to IGCs (interchromatin granule clusters) involved in snRNP (small nuclear ribonucleoprotein) assembly, maturation and storage; and in CBs that are nuclear domains for snRNP modification and maturation, amongst

[1] Dedicated to our late colleague and friend M.E. Fernández-Gómez (28/03/2007).

[2] To whom correspondence should be addressed (email smoreno@cib.csic.es).

**Key words:** germination, nuclear organization, splicing factors, tomato, Z-DNA.

**Abbreviations used:** CB, Cajal body; DAPI, 4′,6-diamidino-2-phenylindole; DFC, dense fibrillar component; dsRNA, double stranded small nuclear RNA; EM, electron microscopy; FC, fibrillar centre; GC, granular component; IG, interchromatin granule; IGC, IG cluster; m3G-snRNA, trimethyl guanosin cap small nuclear RNA; OA, osmium amine; PF, perichromatin fibrils; PG, perichromatin granule; snRNP, small nuclear ribonucleoproteins.

other functions (Lamond and Spector, 2003; Cioce and Lamond, 2005). Nevertheless none of these domains correspond to active co-transcriptional splicing sites, as they do not contain pre-mRNAs, and most active genes localize at the perichromatin compartment where snRNPs associate with pre-mRNAs during elongation (Fakan, 2004). The PFs (perichromatin fibres) correspond to newly synthesized pre-mRNAs, whereas PGs (perichromatin granules) are pre-mRNAs storing particles. Besides the perichromatin compartment, the snRNPs mostly localize to the IGCs, corresponding to the speckles observed by immunofluorescence (Fakan, 2004).

The organization of endogenous spliceosomal components in plant nuclei has been analysed in several species by immunolabelling with antibodies against different conserved splicing factors, such as U2B″, Sm and SR (Ser/Arg-rich splicing) proteins (Vázquez-Nin et al., 1992, Glyn and Leitch, 1995; Boudonck et al., 1998; Acevedo et al., 2002b; Cui and Moreno Díaz de la Espina, 2003; Docquier et al., 2004), and by expression of GFP (green fluorescent protein)-fusion proteins in living cells (Docquier et al., 2004, Fang et al., 2004; Lorkovic et al., 2004; Tillemans et al., 2006).

Early immunofluorescence studies in proliferating cells showed two labelled compartments in plants: the CBs and a diffuse interchromatin network (Glyn and Leitch, 1995; Boudonck et al., 1998; Acevedo et al., 2002b; Cui and Moreno Díaz de la Espina, 2003). Previously the localization of SR proteins, a marker of nuclear speckles, evidenced the presence of different subpopulations of nuclear speckles in plants with a dynamic organization related to transcriptional levels (Lorkovic and Barta, 2004; Lorkovic et al., 2004; Fang et al., 2004; Tillemans et al., 2006).

Plant CBs have been characterized in different species as being similar to vertebrate CBs (Moreno Díaz de la Espina et al., 1982; Glyn and Leitch, 1995; Boudonck et al., 1998; Acevedo et al., 2002b; Cui and Moreno Díaz de la Espina, 2003), in spite of the very low similarity between Atcoilin and the marker protein of vertebrate CBs (Collier et al., 2006), and they also have a role in siRNA (small intefering RNA) assembly (Li et al., 2006). The main RNP structures filling the interchromatin domains in plants are IGs (interchromatin granules). Plant IGs form an interchromatin loose network, but not large IGCs as observed in animal cells (Medina et al., 1989; Moreno Díaz de la Espina et al., 1992; Fang et al., 2004). Co-transcriptional splicing has been demonstrated in mildly dispersed tomato meristematic nuclei (Vázquez-Nin et al., 1992).

Distributions of splicing factors in plant nuclei vary according with the species, tissue and metabolic activity (Glyn and Leitch, 1995, Acevedo et al., 2002b, Cui and Moreno Díaz de la Espina, 2003; Lorkovic and Barta, 2004; Fang et al., 2004). Their evolution during activation of quiescent roots was analysed in radicle bands of sugarcane stems (Acevedo et al., 2002b), onion bulbs (Cui and Moreno Díaz de la Espina, 2003), and maize and *Arabidopsis* seeds (Docquier et al., 2004). The quiescent splicing factors are stored in CBs associated to the nucleolus in sugarcane (Acevedo et al., 2002b) or in nucleoplasmic microspeckles in the other species (Cui and Moreno Díaz de la Espina, 2003; Docquier et al., 2004). During activation, splicing factors redistribute to the nucleoplasmic CBs and also to a diffuse nucleoplasmic network (Acevedo et al., 2002b; Cui and Moreno Diaz de la Espina, 2003).

Embryos of seeds have a programmed transition from quiescence to cell proliferation during germination that starts with water uptake by the seed and ends with the protrusion of the radicle from the seed coat. Germination is a well-characterized and complex process, and the cells of the quiescent radicle constitute a very good system to analyse nuclear evolution from a dehydrated practically inactive state, to the steady state of proliferation. Seeds contain large amounts of mRNA species, both spliced and unspliced, that are used in early germination protein synthesis (Bewley, 1997; Sheoran et al., 2005; Nakabayashi et al., 2005). The organization of splicing components during seed germination and post-germination events has been studied in maize and *Arabidopsis* (Docquier et al., 2004).

In the present study, we looked at nuclei from the radicle blastema during germination and from active meristems in post-germinating growing roots of tomato (*Lycopersicon esculentum*) to analyse the relationships between the ultrastructural changes in the different nuclear domains, mainly the process of chromatin decondensation and evolution of nuclear RNPs, and the spatial and temporal organization of transcription and splicing factors in nuclei. *L. esculentum* is a dicot with a very low 2C DNA content (1.96 pg) and chromocentric chromatin organization

(Dolezel and Bartos, 2005; Lingua et al., 2002) like *Arabidopsis*, but their nuclei are much more adequate for *in situ* analysis and their seeds are easier to manipulate. Besides, the nuclear ultrastructure and RNP organization of steady state tomato meristematic cells in growing roots is well characterized (Moreno Díaz de la Espina et al., 1992; Vázquez-Nin et al., 1992) and the germination process is well documented (de Castro et al., 2000; Sheoran et al., 2005).

## Results

### Organization of the quiescent nucleus

Cells from the radicle blastema of dry seeds appeared highly vacuolated by EM (electron microscopy). Their dense nuclei were small with ruffled outlines compared with those in the steady state meristems of the merged radicle (Figure 1a). They displayed highly compacted chromatin masses and reticulated interchromatin regions by both EM (Figure 1) and DAPI (4′,6-diamidino-2-phenylindole) staining for confocal microscopy (Figures 2a and 3a′). No extended chromatin was observed by OA (osmium amine) specific contrast for EM. Within the uncontrasted nucleolus, condensed chromatin aggregates similar to NORs (nucleolar organizer regions) (Acevedo et al., 2002a) were evident (Figure 1b). EDTA preferential staining for RNPs demonstrated a compact round nucleolus with a dense fibrillar organization displaying bleached NORs, but lacking distinct nucleolar FCs (fibrillar centres) and GCs (granular components) (Figure 1c). The densely packed interchromatin regions were adjacent to the nucleolus and appeared crowded with RNP structures, mainly IGs (Figures 1c and 1d).

As *in situ* run-on transcription assays are impossible in dry seeds, and not reliable in partially hydrated early germinating cells, we performed immunolabelling of the Z-DNA stretches formed after the active RNA polymerases as a marker for transcription (Wittig et al., 1992; Černá et al., 2004). Z-DNA labelling was essentially negative in dry radicle nuclei (Figures 2a and 2a′), in agreement with the densely packed organization of their chromatin after OA staining (Figure 1b). Both results suggested that quiescent nuclei in the dry seed were inactive in transcription.

In quiescent nuclei, U2B″ and Sm proteins were mostly stored in large nucleolus-associated-CBs, as revealed by 4G3 and Y12 immunofluorescence (Figures 3a, 3a′, 3c and 3c′). Most nuclei showed a single labelled CB, approx. 30% of the nuclei presented no reactive CBs and a few nuclei showed a very faint diffuse interchromatin labelling, much weaker than that of the CBs (Figures 3a and 3c). Most CBs were spherical, but flattened and hollow-sphere-shaped ones were also seen (Figsures 3a and 3c). The labelling obtained with the two sera was similar, but due to space limitations, only the results with U2B″ are presented.

### Reorganization of nuclear domains during germination

In early germination, radicle cells reassume basic metabolism by water imbibition. Their nuclei progressively became spherical or ellipsoidal. This process was accompanied by the de-compaction of the chromatin clumps, giving rise to compact chromatin masses of different sizes, the bigger ones associated with the nuclear envelope, as revealed by OA staining (data not shown). After 4 h of soaking, few changes were observed in the nucleoplasmic RNP-containing structures, which appeared sparsely distributed in the expanding interchromatin domains. The nucleolus presented a dense compact fibrillar organization, typical of inactive states (Figure 4a; Acevedo et al., 2002a). The large perinucleolar CBs appeared sometimes flattened (Figure 4a, inset panel). After 9 h of imbibition, variations in nuclear organization were evident at the EM. Chromatin de-condensation was more advanced (Figure 4b). After EDTA preferential staining, the interchromatin domains displayed scarce PGs and RNP-containing fibrils, and the nucleolus became progressively unravelled (Figure 4c).

### Distribution of Z-DNA stretches and splicing factors

Immunofluorescence localization of Z-DNA demonstrated that imbibited nuclei were asynchronous, and very few nuclei presented Z-DNA stretches associated with active RNA polymerases in the first hours (Figure 2c). A large nucleolar signal was the only labelling detected using this approach during the first 3 h of imbibition (Figures 2a′–2c′). The Z-DNA signal then dispersed within the unravelling nucleolus (Figures 2d′ and 4c), which also occurs with the ribosomal genes during soaking (Acevedo et al., 2002a). The label extended into the expanding

**Figure 1 | Ultrastructure of quiescent nuclei in the radicle blastema**

(**a**) Uranyl acetate and lead citrate EM staining. Radicle cells display small and dense nuclei with ruffled outlines and crowded cytoplasm with plenty of storing organelles. The shrunk and dense nucleoplasm shows continuity with the compact fibrillar nucleolus. The clumps of condensed chromatin associated with the nuclear envelope show lower contrast than the RNP containing structures. Bar = 2 μm. (**b**) OA-specific staining for DNA displays heavily contrasted compact chromatin aggregates, opposed to the nuclear envelope, and inside the uncontrasted nucleolus (no). No decondensed chromatin fibres are evident. Bar = 200 nm. (**c**) and (**d**) EDTA method for RNPs. (**c**) The dense fibrillar nucleolus (no) and the reticulated interchromatin regions (ir) appear contrasted, but not the clumps of condensed chromatin (arrow). The nuclear RNPs stand out in the interchromatin regions. Bar = 500 nm. (**d**) Interchromatin domains with deeply stained IGs and fibres (arrow). Bar = 400 nm.

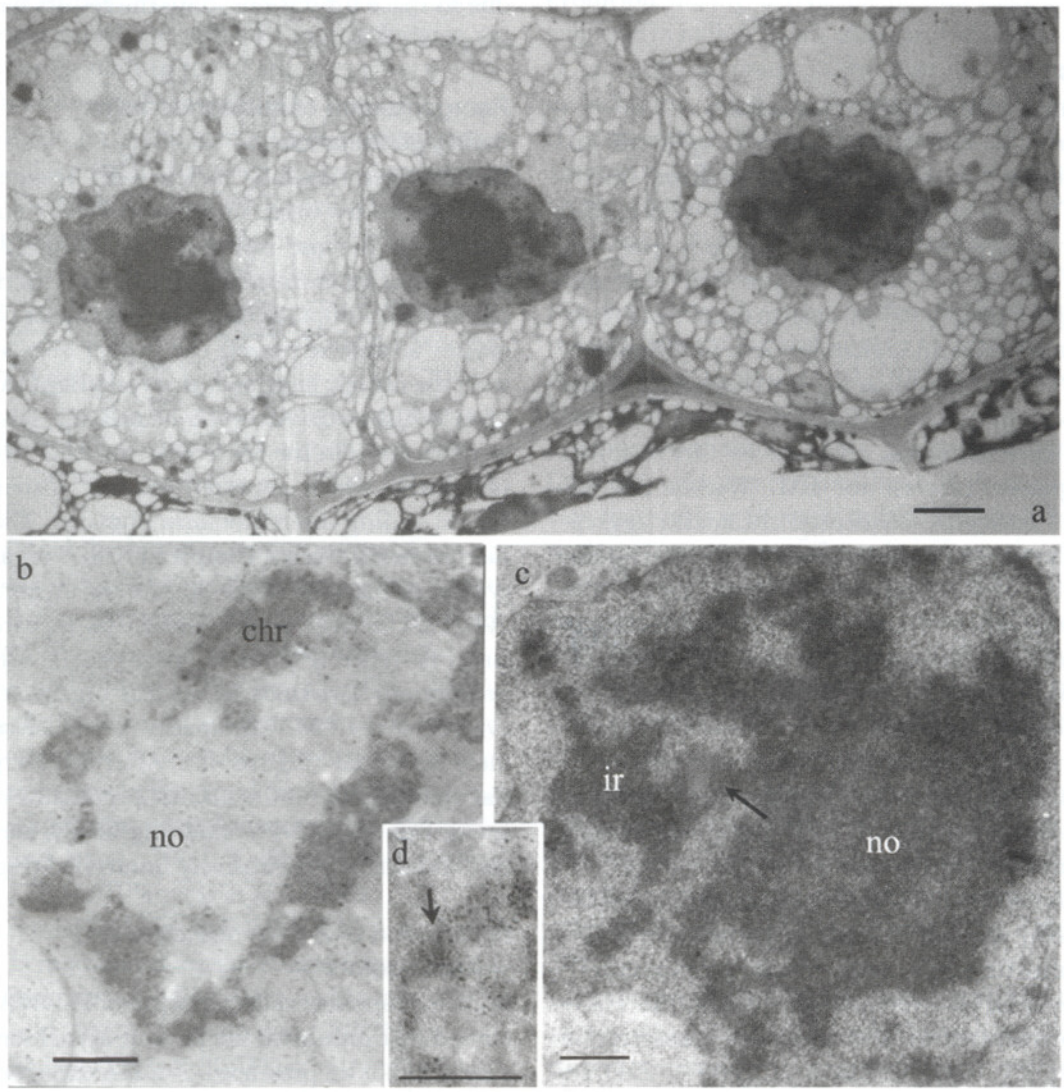


interchromatin regions starting in small weak foci (Figures 2d′ and e′). After 9 h of soaking, the Z-DNA signal increased in the interchromatin regions, where spots of higher intensity were frequently observed, probably reflecting the clustering of gene expression during this period (Nakabayashi et al., 2005). The nucleolar signal appeared spread, which also occurred with the FCs (Figure 4e), except for some areas probably corresponding to the GC and cavity (Figures 2f′ and 2g′).

**Figure 2 | Localization of Z-DNA stretches by immunofluorescence during germination**
(**a′**) Quiescent dry seeds. (**b′–f′**) Germinating seeds after different imbibition times as indicated in figures. (**g′**) Proliferating meristematic cells in growing roots. (**a–g**) Overlays of DAPI and anti-Z-DNA stainings. No signal was detected in quiescent nuclei (**a′**). In early germination a single intense nucleolar spot was detected (**b′** and **c′**). After 4 h imbibition the nucleolar labelling spreads throughout the nucleolar body (**d′**). After 6 h, the labelling increases in the developing interchromatin domains that display some bright spots (**e′**). At 36 h after soaking the nucleolus and the loose interchromatin regions depict an intense labelling throughout (**f′**) similar to that in the meristems of growing roots with a diffuse nucleolar and nucleoplasmic labelling with some bright spots (**g′**). The labelling associated to the inner nuclear envelope in these cells, probably corresponds to dsRNA. Bars = 8 μm.

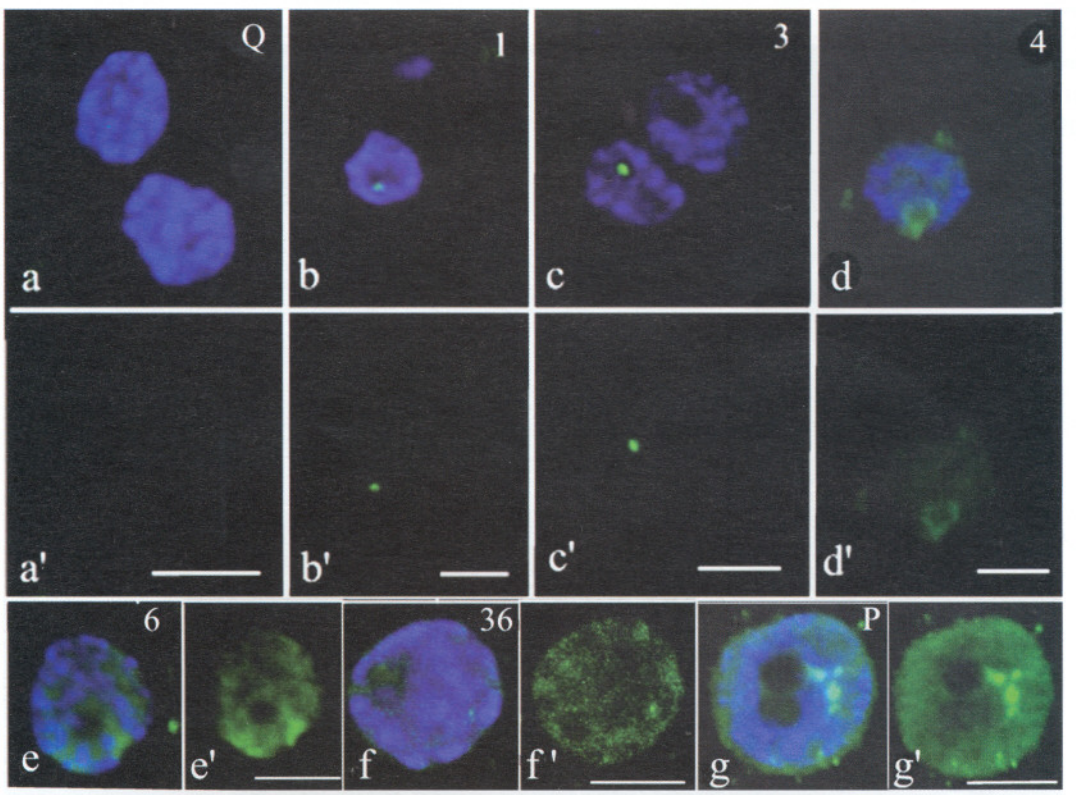


After 1 h of soaking, the U2B″ and Y12 stainings in CBs were similar to those in unsoaked nuclei (Figures 3a, 3c and 3d). During the second hour, the expanding interchromatin regions showed a diffuse labelling in some nuclei before any transcription was detected by immunofluorescence (Figure 3e), suggesting that the signal corresponds to the relocation of splicing proteins, but not to co-transcriptional splicing. This trend continues steadily; however, there were important variations between different cells in the blastema due to their asynchrony (de Castro et al., 2000). From hours 4 to 9 of imbibition, both anti-U2B″ and anti-Y12 labelling demonstrated highly contrasted perinucleolar CBs (Figures 3f and 3h), that frequently showed flattened and hollow-sphere shapes (Figures 3g and 3h). A single labelled CB was most frequently observed during early germination. The frequency of nuclei with two or three CBs increased slowly until the steady state of proliferation in which nuclei have up to 10 CBs (Figures 3j, 4e and Supplementary Figure 1 at http://www.biolcell.org/boc/099/boc0990519add.htm). These preparations also revealed the formation of transient speckles of different sizes in the interchromatin regions of some nuclei (Figure 3).

**Figure 3 | Nuclear compartmentalization of splicing factors during radicle germination**

(**a–j**) U2B″ immunofluorescence. (**a′–j′**) Overlays of the DAPI and U2B″ signals. (**a′** and **c′**) Small quiescent radicle nuclei with ruffled outlines. The condensed chromatin fills most of the nuclear volume. In quiescent cells (**a** and **c**) and very early germination (**d**) the U2B″ protein mostly accumulates in nucleolus-associated CBs, with occasional weak diffuse nucleoplasmic labelling. Note the heterogeneity of U2B″ distribution amongst cells of the radicle. Later on the protein accumulates in CBs but also display a diffuse or speckled cytoplasmic staining (**e** and **f**). In more advanced germination, the protein becomes progressively enriched in the nucleoplasm sometimes forming a kind of microspeckles besides the bright CBs (**g–i**). (**b′** and **j′**) Proliferating meristematic large spherical nuclei from growing roots with the usual distribution of U2B″ protein in numerous small nucleoplasmic CBs and a diffuse nucleoplasmic staining without speckles (**b** and **j**). The large nucleoli appear as dark spots after DAPI staining. Bars = 8 μm.

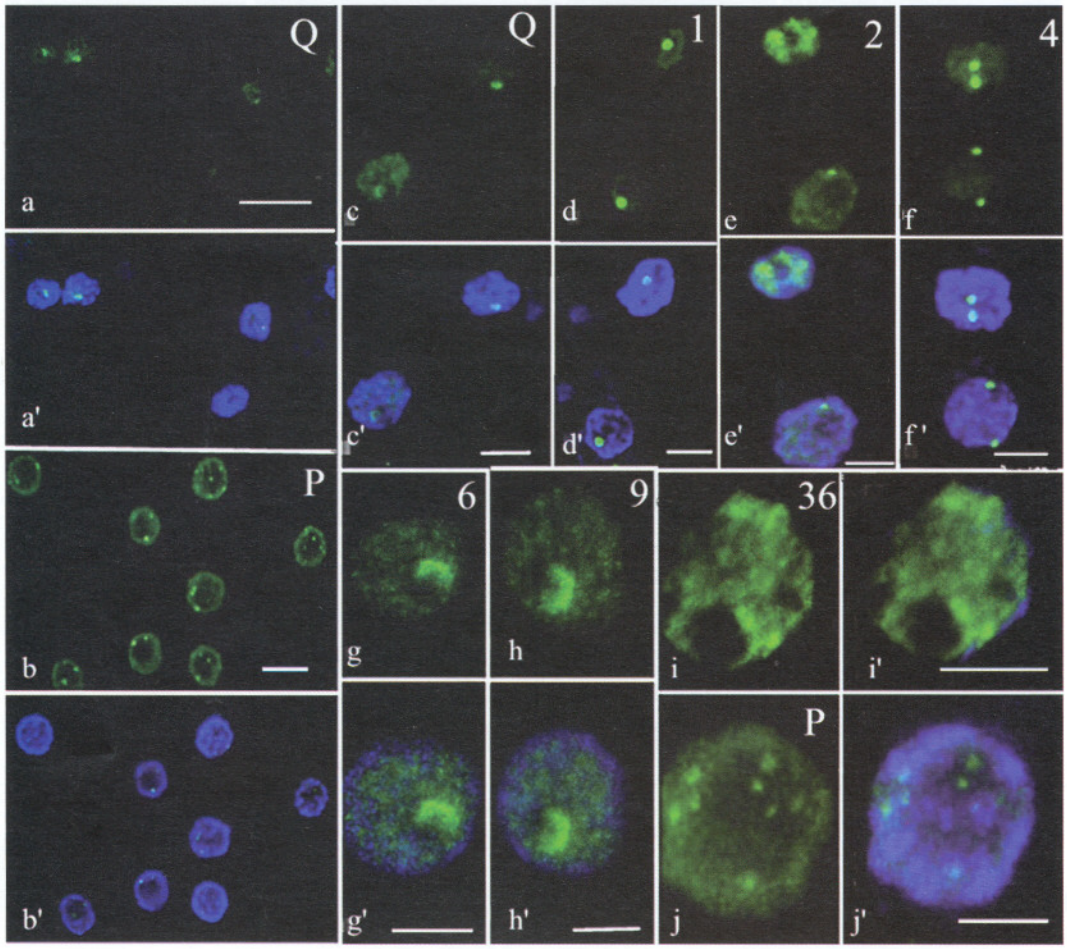


## Nuclear organization of proliferating roots after germination

Meristematic nuclei from active growing roots were ellipsoidal with smooth outlines and depicted one or two large and loose nucleoli, with small clear FCs dispersed in the DFC (dense fibrillar component) around them, and a well-developed GC. A nucleolar cavity was very frequently observed at this stage (Figure 4e). Condensed chromocentres associated with the nuclear envelope, with the typical distribution of this species evidenced after OA-specific staining that also revealed small chromatin patches and decondensed fibres (Figure 4d). The extended and clear nucleoplasm contained abundant RNP particles throughout, including sparse IGs and fibrils, as well as numerous nucleoplasmic CBs, which were smaller than those associated with the nucleolus during germination (Figure 4e).

**Figure 4 | Nuclear ultrastructure in germinating and steady-state-meristematic radicle cells**
(**a**) After 4 h of imbibition. (**b** and **c**) After 9 h of imbibition. (**d–h**) Steady state proliferating cells in growing roots. (**a**) Uranyl acetate and lead citrate staining. Compact fibrillar nucleolus (no) with an associated CB. Bar = 100 nm. The inset panel illustrates a flattened CB. Bar = 500 nm. (**b**) The OA staining for DNA shows clumps of compact chromatin associated with the nuclear envelope, and small clumps and decondensed chromatin filaments in the nucleoplasm. The nucleolus (no) appears unstained except for some small chromatin aggregates. Bar = 500 nm. (**c**) EDTA staining displaying the distribution of nuclear RNPs. Nucleolus (no) with an extended configuration characteristic of activity. RNP-containing fibrils and granules are sparse in the interchromatin region. pcg, perichromatin granule surrounded by a clear halo. Bar = 500 nm. (**d**) OA staining of meristematic nuclei reveals the chromocentres apposed to the nuclear envelope, but also small chromatin clumps and decondensed fibres (arrows) pervading the nucleoplasm and the unstained nucleolus (no). Bar = 2 μm. (**e**) EDTA staining for RNPs displays a contrasted nucleolus (no) with clear FCs surrounded by a highly contrasted DFC and a peripheral GC, CBs free in the nucleoplasm and numerous nucleoplasmic granules. Bar = 2 μm. (**f–h**) Immunogold labelling of splicing components. (**f** and **h**) Localization of m3G-snRNAs in a CB and in the peri- and inter-chromatin regions (**h**), but not in the nucleolus (no) Bars in **d–f** = 100 nm. (**g**) Sm proteins recognized by Y12 serum in the CB. A group of gold grains decorating a nucleoplasmic fibril (arrow) Bar = 200 nm.

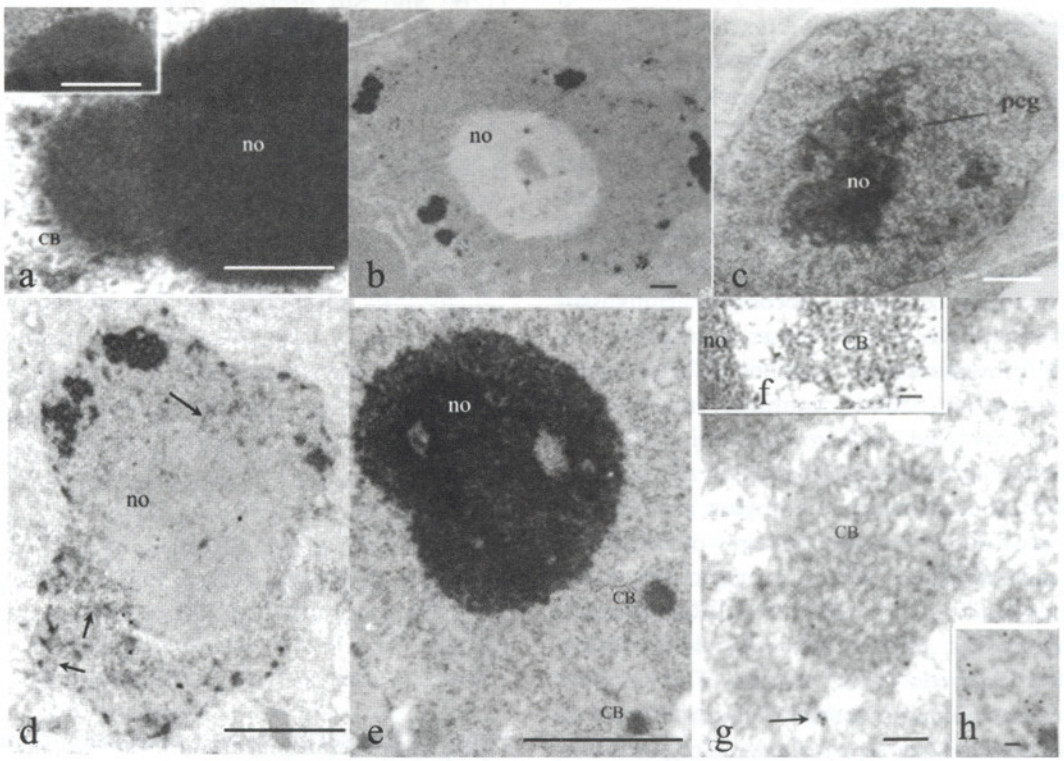


The anti-Z-DNA signal was high in steady state proliferating nuclei. It appeared widely distributed in the interchromatin domains, where bright spots of different sizes were found (Figures 2g and 2g′). The nucleoli displayed a diffuse signal (Figures 2g and 2g′), corresponding to the decondensed state of their chromatin detected by OA staining (Figure 4d) and also non-reactive regions, mostly corresponding to the GC (Figure 4e). These nuclei also presented a peripheral Z-DNA signal associated with the nuclear envelope, which was not present in the earlier stages of germination (Figures 2g and 2g′), probably corresponding to dsRNAs (Rich and Zhang, 2003; A. Černá, S. Moreno Díaz de la Espina, A. Cuadrado, N. Jouve and C. de la Torre, unpublished data).

U2B″ and Y12 immunofluorescence signals were higher than during germination (Figure 3). The nuclei depicted a diffuse labelling in the wide interchromatin domains and also numerous (1–10) bright CBs,

either perinucleolar or nucleoplasmic (Figures 3j, 3j′ and Supplementary Figure 1).

The immunogold localization of Sm proteins and the m3G-snRNAs (trimethyl guanosin cap small nuclear RNAs) demonstrated the presence of snRNAs in CBs (Figures 4f and 4g) and also in the nucleoplasm associated with perichromatin fibrils (Figure 4h), whereas the nucleolus appeared devoid of gold grains (Figure 4f).

## Discussion

### Ultrastructural compartmentalization in nuclei from resting radicle cells

The results of EM showed that dehydration during tomato seed maturation induces an extreme reduction in nuclear size and a severe collapse and redistribution of the main nuclear domains (Moreno Díaz de la Espina et al., 1992). Resting radicle blastema nuclei show the typical organization of quiescent tissues with very low water contents and standstill metabolic activity. Their chromatin condensation is almost complete as revealed by both DAPI and OA staining. The absence of Z-DNA conformations associated with active RNA polymerases, detected by the sensitive immunofluorescent method (Wittig et al., 1992; Černá et al., 2004), confirms transcription arrest in the dry seed, in agreement with the biochemical results (Bewley, 1997; Bove et al., 2001).

The RNP domains form a compact continuum. The nucleolus depicts typical features of metabolic inactivity: a very dense fibrillar structure, the ribosomal genes condensed in compact NORs instead of forming active FCs, and lack of canonical GCs (Bassy et al., 2000; Acevedo et al., 2002a). The compact interchromatin domains contain a high density of RNP structures and display a reticulated organization in contrast with their loose distribution in active cells (Moreno Díaz de la Espina et al., 1992). Similar nuclear features, although not so extreme, were found in quiescent tissues with higher hydration levels, such as sugarcane stems (Acevedo et al., 2002b), onion root meristems of bulbs (Risueño and Moreno Díaz de la Espina, 1979), and in maize and *Arabidopsis* seeds (Docquier et al., 2004).

### Storing domains for splicing factors in resting nuclei

In tomato quiescent radicle nuclei, immunofluorescence demonstrated the compartmentalization of U2B″ and Sm proteins mostly in nucleolar CBs, which has also been observed in dormant root primordia of sugarcane (Acevedo et al., 2002b). In contrast, in quiescent nuclei of onion roots that lack nucleolar CBs, the splicing factors accumulate in nucleoplasmic microspeckles (Cui and Moreno Díaz de la Espina, 2003). This is also seen in resting roots of maize and *Arabidopsis* seeds that have nucleolar CBs; however, the U2B″ protein and the U1/U6 snRNAs are not stored in them (Docquier et al., 2004). The available data of immunofluorescence, flow cytometry (Dolezel and Bartos, 2005; Acevedo et al., 2002a), chromatin organization (Lingua et al., 2002) and taxonomy indicate that the pattern of nuclear compartmentalization of extant splicing components in plants in either CBs or microspeckles, is not related to genome size, condensed chromatin pattern or taxonomic position (Figure 2 and Table 1). The molecular mechanism underlying this compartmentalization remains unknown.

**Table 1 | Compartmentalization patterns of extant splicing factors in several dicot and monocots differing in DNA content and chromatin organization**

| Species | 2C DNA content (pg) | Chromatin organization | Extant splicing factors | D/m |
|---|---|---|---|---|
| *A. thaliana* | 1.08* | Chromocentric | Microspeckles | D |
| *L. esculentum* | 1.96* | Chromocentric | Nucleolar CBs | D |
| *Z. mays* | 5.72* | Reticulate | Microspeckles | M |
| *S. officinarum* | 6† | Semi-reticulate | Nucleolar CBs | M |
| *A. cepa* | 35* | Reticulate | Microspeckles | M |

*Dolezel and Bartos (2005).
†Acevedo et al. (2002a).

### Firing of transcription and evolution of nuclear domains during germination

The Z-DNA conformation is not a stable feature of double helix DNA, but a transient structure occasionally induced by biological activity. The existence of specific Z-DNA-binding proteins and its formation during nucleosome remodelling demonstrate its physiological role (Rich and Zhang, 2003). Studies in permeabilized mammalian nuclei have demonstrated a transient formation of Z-DNA stretches behind active RNA polymerases near gene promoters that correlates with transcription levels (Wittig et al., 1992; Rich and Zhang, 2003). Z-DNA immunofluorescence in isolated nuclei from proliferative onion roots

demonstrated the reliability and sensitivity of this *in situ* approach in plants (Černá et al., 2004).

The present Z-DNA immunolabelling results demonstrate the transcriptional arrest of quiescent roots and allow an early detection of transcription, not detectable by biochemical analysis, in the precocious subset of the asynchronous meristematic cell population (De Castro et al., 2000). They also demonstrate that the onset of nucleolar transcription is previous to any mRNA synthesis, in agreement with the biochemical analyses (Bewley, 1977). The nucleolar Z-DNA signal is compact in early stages of germination because rRNA synthesis occurs associated to the condensed NORs, but later the ribosomal genes unravel and the signal becomes spread in the nucleolus excluding the GC domain that contains the preribosomal particles and does not sustain transcription (Bassy et al., 2000; Acevedo et al., 2002a).

The EM and immunofluorescence results suggest that the chromatin de-condensation, and the increase in size and rearrangement of the interchromatin domains of early germination are caused by the reassumption of cell metabolic activity after hydration, and take place before the onset of mRNA synthesis. This agrees with the resistance to α-amanitin of early germination, but not of the subsequent seedling growth, whereas cycloheximide treatment blocks germination (Rajjou et al., 2004).

Tomato nuclei from dry radicles do not have speckles. During germination speckles are observed only in a small fraction of cells, indicating that they are transient structures formed during nuclear reactivation. The splicing proteins would later relocate from speckles to the diffuse nucleoplasmic network or free CBs. The germination speckles have a different organization from those in differentiated polyploid cells of the same roots (data not shown) and also from the microspeckles of quiescent nuclei (Cui and Moreno Díaz de la Espina, 2003) and from those containing SR proteins in other plants (Lorkovic and Barta, 2004; Lorkovic et al., 2004; Fang et al., 2004; Docquier et al., 2004). These observations confirm previous data on the heterogeneity of speckles in plant cells (Lorkovic and Barta, 2004).

These results together indicate that the nuclear RNA components in the dry radicle nuclei are similar to those in the mature seed and are stored in the collapsed interchromatin domains. The early formation of microspeckles would correspond to a rearrangement or maturation of pre-existing RNP components, rather than to synthesis of new RNAs, highlighting the role of extant RNAs in the process.

The ultrastructural re-arrangements observed during early imbibition such as the changes in nuclear shape and size, the massive chromatin de-condensation and the progressive unravelling of the nucleolus and interchromatin domains, are pre-requisites for the initiation of transcription. They also take place during activation of $G_0$ in cells of the root meristems of onion bulbs (Bassy et al., 2000) and sugarcane stems (Acevedo et al., 2002a).

The initiation of transcription is one of the major events of the phase I of germination, allowing the synthesis of new mRNA coding for proteins necessary for seed maturation (Bewley, 1997; Bove et al., 2001). Our data demonstrate activation of nucleolar transcription approx. 3 h before the beginning of any mRNA transcription that would provide ribosomes for resumption of translation upon imbibition (Bewley, 1997). The protein synthesis that takes place several hours before new mRNAs are available in the radicle uses extant mRNAs from seeds that contain thousands of stored mRNA species (Nakabayashi et al., 2005). These would be stored as RNP granules in the crowded interchromatin domains of resting nuclei. The timing of mRNA synthesis obtained by Z-DNA labelling during germination correlates with the mRNA profile obtained in dry and imbibited *Arabidopsis* seeds by microarrays, which detected a different transcriptome as early as 6 h after imbibition (Nakabayashi et al., 2005).

Thus the early rearrangement of splicing components from CBs to interchromatin domains, previous to the firing of mRNA synthesis, would be independent of transcription. It could be related more to events involved in maturation and early recruitment of the splicing machinery for splicing of stored mRNAs, than to the preparations for the initiation of co-transcriptional splicing (Vázquez-Nín et al., 1992).

The initiation of events associated with activation, such as relocation of the splicing components from CBs to the interchromatin regions and initiation of transcription do not occur synchronously in the radicle. They start in very few cells and then extend progressively to the rest of the cell population. This asynchrony may be due to shortness of ATP, because of a decline in respiration, probably due to rate of

diffusion of the oxygen through the structures surrounding the radicle; to a different rate of hydration within the tissue (Bewley, 1997) or to the asynchrony of the cell population (De Castro et al., 2000).

Z-DNA immunolabelling revealed a redistribution of the nucleolar transcription sites along tomato radicle germination typical of high activity (Bassy et al., 2000; Acevedo et al., 2002a) accompanied by the onset of nucleoplasmic mRNA synthesis. Concomitantly there is an accumulation of splicing components in the interchromatin region. During this period scarce RNP particles are detectable in the interchromatin region by EM after EDTA staining. The early mRNA synthesis correlates with the visualization of newly synthesized and processed mRNAs in the form of perichromatin granules, which is found in some meristematic nuclei 5 h after the extra-nucleolar transcription started.

### CBs are the main nuclear domains for storage of splicing factors in tomato seeds

Our results demonstrate a role of nucleolus-associated CBs in long-term storage of splicing components synthesized before seed desiccation, and a later transcription-independent recruitment of these components to the interchromatin domains, probably related to maturation and/or recruitment of the splicing machinery for processing of extant mRNAs necessary for resumption of metabolic activity (Bove et al., 2001). This mechanism was also observed in quiescent radicle bands of the monocot sugarcane (Acevedo et al., 2002b). In other dicot and monocot species, the long-term storing of splicing factors occurs in nucleoplasmic microspeckles that relocate to CBs only after imbibition (Cui and Moreno Díaz de la Espina, 2003; Docquier et al., 2004) indicating the complexity of the nuclear processes involved in seed germination.

The numbers of CBs increase during metabolic activation in several plant dormant tissues: sugarcane root primordia (Acevedo et al., 2002a; 2002b), onion bulb root blastema (Cui and Moreno Díaz de la Espina, 2003), *Arabidopsis* root epidermis (Boudonck et al., 1998), and tomato embryonic cells (the present study). However, in maize, the numbers of CBs do not change in meristematic cortical cells during the first 72 h of germination and decreases afterwards (Docquier et al., 2004). These variations may be due to differences in the processes of nuclear activation or to dynamic and other intrinsic properties of CBs (Collier et al., 2006). All these observations confirm that the numbers and sizes of CBs are not reliable parameters to be used as general markers of metabolic activation during germination.

### Meristematic roots cells after germination

Soon after post-germination the nuclear structures as well as the organization of transcription and splicing resemble that of fully active steady-state meristems in growing roots (Moreno Díaz de la Espina et al., 1992; Acevedo et al., 2002b; Cui and Moreno Diaz de la Espina, 2003). The steady state proliferating nuclei of active roots have nuclear anti-Z-DNA staining associated with the inner nuclear membrane, probably corresponding to accumulation of RNAs containing double strand regions on their way to the cytoplasm (Rich and Zhang, 2003; Černá et al., 2004; A. Černá, S. Moreno Díaz de la Espina, A. Cuadrado, N. Jouve and C. de la Torre, unpublished data) that was not observed in nuclei of dry seeds or germinating radicles, revealing a low rate of extranucleolar RNA synthesis and storage during these periods.

## Materials and methods

Radicles of tomato (*Lycopersicon esculentum* var. Heing) seeds were excised from dry seeds or after 1, 2, 4, 6, 9 or 36 h of imbibition on moist filter paper in a Petri dish at room temperature (24°C). Steady state proliferative meristematic cells of growing roots were used as active metabolic controls.

### EM

For conventional EM, samples were fixed in 4% (w/v) paraformaldehyde and 2% (v/v) glutaraldehyde in 0.025 M phosphate buffer (pH 7.2) for 1 h at room temperature, rinsed in the same buffer, dehydrated in ethanol, and then embedded in Glycide ether 100 (Merck, Darmstadt, Germany). For staining of RNP structures, Bernhard's EDTA staining was performed as described previously (Moreno Díaz de la Espina et al., 1992). DNA-containing structures were stained using the OA procedure modified by Vázquez-Nin and co-workers (1995).

For immunoelectron microscopy samples were fixed in 4% (w/v) paraformaldehyde in PBS for 1 h at 4°C and embedded in LRWhite resin polymerized at 50°C. Immunolocalizations were performed on thin sections using the method described previously (Vázquez-Nín et al., 1992). As controls, grids were incubated in the same conditions without primary antibody. Observations were made using Zeiss EM10 and JEOL 1010 microscopes.

### Immunofluorescence

Samples were fixed in 4% (w/v) paraformaldehyde in PBS for 1 h at 4°C, digested with 2% (w/v) cellulase and 20% (w/v) pectinase for 50 min at 37°C in MAN buffer (pH 7.0) and processed as described by Acevedo et al. (2002b). The antibodies used in the

**Table 2 | Antibodies used in the present study**
Ab, antibody.

| Primary Ab (Catalogue #) | Origin | Company | Secondary Ab | Label |
|---|---|---|---|---|
| Anti-U2B″ (4G3) | Mouse monoclonal | Organon | GAM | Alexa Fluor® 488 |
| Anti-Sm (Y12) | Mouse monoclonal | NeoMarkers | GAM | Alexa Fluor® 488 or Alexa Fluor®546 |
| Anti-m3G-snRNA (R1131) | Rabbit polyclonal | Oncogene | GAR | 5-10 nm gold |
| Anti Z-DNA | Sheep polyclonal | Abcam | RAS | FITC |

present study are shown in Table 2. Preparations were examined using a confocal microscope Leica TCS-SP2-AOBS-UV with a 63×, 1.4 NA oil immersion objective.

## Acknowledgements

This work was supported by Spanish DGI project BFU 2006-00379 and by a CSIC-UNAM agreement for academic interchange. We thank M. Carnota for skilful technical assistance. O.E. and G.V.N. thank DGAPA (La Dirección General de Asuntos del Personal Académico; UNAM) for support during the sabbatical leave.

## References

Acevedo, R., Cuadrado, A., De la Torre, C. and Moreno Díaz de la Espina, S. (2002a) Behaviour of ribosomal genes and nucleolar domains during activation in sugarcane (*Saccharum officinarum* L.) root primordia: from the unsoaked quiescent state to the steady state of proliferation. Eur. J. Histochem. **46**, 143–158

Acevedo, R., Samaniego, R. and Moreno Díaz de la Espina, S. (2002b) Coiled bodies in nuclei from cells evolving from dormancy to proliferation. Chromosoma **110**, 559–569

Bassy, O., Jiménez-García, L.F., Echeverría, O.M., Vázquez-Nin, G.H. and Moreno Díaz de la Espina, S. (2000) High resolution detection of rRNA and rDNA in plant nucleoli with different activities by *in situ* hybridization. Biol. Cell **92**, 59–70

Bewley, J.D. (1997) Seed germination and dormancy. Plant Cell **9**, 1055–1066

Boudonck, K., Dolan, L. and Shaw, P. (1998) Coiled body number in the *Arabidopsis* root epidermis are regulated by cell type, developmental stage and cell cycle parameters. J. Cell Sci. **111**, 3687–3694

Bove, J., Jullien, M. and Grappin, Ph. (2001) Functional genomics in the study of seed germination. Genome Biol. **3**, 1002.1–1002.5

Černá, A., Cuadrado, A., Jouve, N., Moreno Díaz de la Espina, S. and De la Torre, C. (2004) Z-DNA, a new *in situ* marker for transcription. Eur. J. Histochem. **48**, 49–56

Cioce, M. and Lamond, A.I. (2005) Cajal bodies: a long history of discovery. Annu. Rev. Cell. Dev. Biol. **21**, 105–131

Collier, S., Pendle, A., Boudonck, K., van Rij, T., Dolan, L. and Shaw, P. (2006) A distant coilin homologue is required for the formation of Cajal bodies in *Arabidopsis*. Mol. Biol. Cell **17**, 2942–2951

Cui, P. and Moreno Díaz de la Espina, S. (2003) Sm and U2B″ proteins redistribute to different nuclear domains in dormant and proliferating onion cells. Planta **217**, 21–31

De Castro, R., van Lammeren, A.A.M., Groot, S.P.C., Bino, R. and Hillorst, H.W.M. (2000) Cell division and subsequent radicle protrusion in tomato seeds are inhibited by osmotic stress, but DNA synthesis and formation of microtubular cytoskeleton are not. Plant Physiol. **122**, 327–335

Docquier, S., Tillemans, V., Deltour, R. and Motte, P. (2004) Nuclear bodies and compartmentalization of pre-mRNA splicing factors in higher plants. Chromosoma **112**, 255–266

Dolezel, Y. and Bartos, J. (2005) Plant DNA flow cytometry and estimation of nuclear genome size. Annals Bot. **95**, 99–110

Fakan, S. (2004) The functional architecture of the nucleus as analysed by ultrastructural cytochemistry. Histochem. Cell Biol. **122**, 83–93

Fang, Y., Hearn, S. and Spector, D.L. (2004) Tissue-specific expression and dynamic organization of SR splicing factors in *Arabidopsis*. Mol. Biol. Cell **15**, 2664–2673

Glyn, M.C.P. and Leitch, A.R. (1995) The distribution of a spliceosome protein in cereal (*Triticeae*) interphase nuclei from cells with different metabolic activities and through the cell cycle. Plant J. **8**, 531–540

Lamond, A.I. and Spector, D. (2003) Nuclear speckles: a model for nuclear organelles. Nat. Rev. Mol. Cell. Biol. **4**, 605–612

Li, C.F., Pontes, O., El-Shami, M., Henderson, I.R., Bernatavichute, Y.V., Chan, S.W.-L., lagrange, T., Pikaard, C.S. and Jacobsen, E. (2006) An ARGONAUTE4-containing nuclear processing center colocalized with Cajal bodies in *Arabidopsis thaliana*. Cell **126**, 93–106

Lingua, G., Fusconi, A. and Berta, G. (2002) The nucleus of differentiated root plant cells: modifications induced by arbuscular mycorrhizal fungi. Eur. J. Histochem. **45**, 9–20

Lorkovic, Z.J. and Barta, A. (2004) Compartmentalization of the splicing machinery in plant cell nuclei. Trends Plant Sci. **9**, 565–568

Lorkovic, Z.J., Hilscher, J. and Barta, A. (2004) Use of fluorescent protein tags to study nuclear organization of the spliceosomal machinery in transiently transformed living plant cells. Mol. Biol. Cell **15**, 3233–3243

Medina, M.A., Moreno Díaz de la Espina, S., Martín, M. and Fernández-Gómez, M.E. (1989) Interchromatin granules in plant nuclei. Biol. Cell **67**, 331–339

Moreno Díaz de la Espina, S., Risueño, M.C. and Medina, F.J. (1982) Ultrastructural cytochemistry and autoradiographic characterization of coiled bodies in the plant cell nucleus. Biol. Cell **44**, 229–238

Moreno Díaz de la Espina, S., Minguez, A., Vázquez-Nin, G.H. and Echeverría, O.M. (1992) Fine structural organization of a non-reticulate nucleus: an ultracytochemical and immunocytochemical study. Chromosoma **101**, 311–321

Nakabayashi, K., Okamoto, M., Kamiya, Y. and Nambar, E. (2005) Genome-wide profiling of stored mRNA in *Arabidopsis thaliana* seed germination: epigenetic and genetic regulation of transcription in seed. Plant J. **41**, 697–709

Rajjou, L., Gallardo, K., Debeaujon, I., Vandekerckhove, J., Job, C. and Job, D. (2004) The effect of α-amanitin on the *Arabidopsis* seed proteome highlights the distinct roles of stored and neosynthesized mRNAs during germination. Plant. Physiol. **134**, 1598–1613

Rich, A. and Zhang, S. (2003) Z-DNA: the long road to biological function. Nat. Rev. Genet. **4**, 566–572

Risueño, M.C. and Moreno Díaz de la Espina, S. (1979) Ultrastructural and cytochemical study of the quiescent root meristematic cell nucleus. J. Submicr. Cytol. **11**, 85–98

Sheoran, I.S., Olson, D.J.H., Ross, A.R.S. and Sawhney, V.K. (2005) Proteoma analysis of embryo and endosperm from germinating tomato seeds. Proteomics **5**, 3752–3764

Spector, D.L. (2001) Nuclear domains. J. Cell Sci. **114**, 2891–2893

Tillemans, V., Leponce, I., Rausin, G., Dispa, L. and Motte, P. (2006) Insights into nuclear organization in plants as revealed by the dynamic distribution of *Arabidopsis* SR splicing factors. Plant Cell. **18**, 3218–3234

Vázquez-Nin, G.H., Echeverría, O.M., Mínguez, A., Moreno Díaz de la Espina, S., Fakan, S. and Martin, T.E. (1992) Ribonucleoprotein components of root meristematic cell nuclei of the tomato characterized by application of mild loosening and immunocytochemistry. Exp. Cell Res. **200**, 431–438

Vázquez-Nin, G.H., Biggiogera, M. and Echeverría, O.M. (1995) Activation of osmium ammine by $SO_2$-generating chemicals for electron microscopy Feulgen-type staining of DNA. Eur. J. Histochem. **39**, 101–106

Wittig, B., Wölfl, S., Dorbic, T., Vahrson, W. and Rich, A. (1992) Transcription of human c-*myc* in permeabilized nuclei is associated with formation of Z-DNA in three discrete regions of the gene. EMBO J. **11**, 4653–4663

Received 16 February 2007/17 April 2007; accepted 18 April 2007

Published as Immediate Publication 18 April 2007, doi:10.1042/BC20070026